Available online at www.sciencedirect.com
SCIENCE DIRECT®
Journal of Solid State Chemistry 178 (2005) 2511–2518
JOURNAL OF SOLID STATE CHEMISTRY
www.elsevier.com/locate/jssc

Connecting small ligands to generate large tubular metal-organic architectures

Andrea M. Goforth, Cheng-Yong Su[1], Rachael Hipp, René B. Macquart, Mark D. Smith, Hans-Conrad zur Loye*

Department of Chemistry and Biochemistry, University of South Carolina, Columbia, SC 29208, USA

Received 16 March 2005; accepted 13 May 2005

Abstract

The new metal-organic framework materials, $ZnF(Am_2TAZ)\cdot$solvents and $ZnF(TAZ)\cdot$solvents (Am_2TAZ = 3,5-diamino-1,2,4-triazole, TAZ = 1,2,4-triazole), have been synthesized solvothermally and structurally characterized by either Rietveld refinement from powder XRD data or by single crystal X-ray diffraction. The three-dimensional structures of the compounds display open-ended, tubular channels, which are constituted of covalently bonded hexanuclear metallamacrocycles ($Zn_6F_6(ligand)_6$). The tubular channels are subsequently covalently joined into a honeycomb-like hexagonal array to generate the three-dimensional porous framework. In the case of $ZnF(Am_2TAZ)\cdot$solvents, hydrophilic $-NH_2$ groups point into the channels, effectively reducing their inner diameter relative to $ZnF(TAZ)\cdot$solvents. The present compounds are isostructural to one another and to the previously reported $ZnF(AmTAZ)\cdot$solvents (AmTAZ = 3-amino-1,2,4-triazole), illustrative of the fact that the internal size and chemical properties of the framework may be altered by modification of the small, heterocyclic ligand. In addition to demonstrating the ability to modify the basic framework, $ZnF(TAZ)\cdot$solvents and $ZnF(Am_2TAZ)\cdot$solvents are two of the most thermally stable coordination frameworks known to date.

Keywords: Rietveld refinement; Thermal stability; Channels

1. Introduction

The exploration of new synthetic strategies targeted at synthesizing novel porous framework materials for applications in the areas of molecular sieves, sensors, gas absorption, ion exchange, size-selective separation and heterogeneous catalysis has engaged researchers for some time now [1]. In particular, efforts have been expended toward the synthesis of new metal-organic frameworks constructed from metal ions and bridging organic ligands. In these systems there are known hurdles to overcome, including the difficulty of controlling pore size and shape, the frequent presence of counterions and solvents within the channels, the tendency to form interpenetrated independent networks, the potential disruption of framework integrity in the absence of guest molecules, and the often low thermal stability of the host framework. To address these potential difficulties, current research has targeted the synthesis of robust open frameworks with high porosity and high thermal stability [2–4], and extensive studies have been carried out on chemical design strategies to enhance the desired properties of the frameworks. Successful approaches include the use of long rigid linkers to increase the spacing between the vertices [5], employing multifunctional bulky organic ligands to prevent interpenetration [6,7], and utilizing secondary building blocks (SBUs) [8] to serve as large vertices. These approaches have created new challenges in the

*Corresponding author. Fax: +1 803 777 8505
E-mail address: zurloye@mail.chem.sc.edu (H.-C. zur Loye).
[1]Permanent address: School of Chemistry and Chemical Engineering, Zhongshan University, Guangzhou 510275, PR China.

0022-4596/$ - see front matter © 2005 Published by Elsevier Inc.
doi:10.1016/j.jssc.2005.05.038

synthesis of tailored organic bridging ligands, in the judicious design of the functional SBUs, as well as in the efficient and synergistic self-assembly of these precursors to generate the desired framework structures. Significant effort has been expended to synthesize long ligands or large SBUs and to achieve non-interpenetrated open framework structures using such ligands and building units. While these efforts have led to some success, certainly when long ligands are used, the thermal stability of such structures is often marginal. Robust SBUs have enjoyed better success and some very thermally stable framework structures have been realized [9].

Recently, we published a structural study of a new, exceptionally stable, hollow tubular metal–organic architecture, [ZnF(AmTAZ)] · solvents (AmTAZ = 3-amino-1,2,4-triazole), which retains its tubular framework structure to an unprecedented 350 °C when heated in air [10]. The large channels in the structure are somewhat of a surprise given the small size of the AmTAZ ligand. In fact, the large channels are not the result of the dimension of the ligand but rather are the result of the metal–ligand connectivities, the metal coordination geometry, and the existence of metal–ligand metallamacrocycles in the structure. Specifically, the ligand–Zn–ligand connectivity, spatially controlled by the location of the nitrogen atoms on the triazole unit, results in $Zn_6(AmTAZ)_6$ rings that are arranged three dimensionally into the channel structure. To further explore this type of framework and to prepare related structures, we opted to modify the ligand used in the synthesis, thereby affecting the number and type of functional groups protruding into the channels. Consequently, features of the channel, such as the degree of hydrophobicity or the interior topology, can be altered while still maintaining the overall framework structure.

One can readily envision modifying the AmTAZ ligand, used for the synthesis of [ZnF(AmTAZ)] · solvents and shown in Scheme 1, by either removing the amino group to generate the 1,2,4-triazole (TAZ) ligand or by adding an additional amino group, to form the 3,5-diamino-1,2,4-triazole (Am_2TAZ) ligand. We used these two ligands, Am_2TAZ and TAZ, to synthesize isomorphic framework structures in which the channel environment has been modified, yet where the high thermal stability has been retained. In this paper we describe the synthesis, structural characterization and significant thermal stability of ZnF(TAZ) · solvents and ZnF(Am_2TAZ) · solvents.

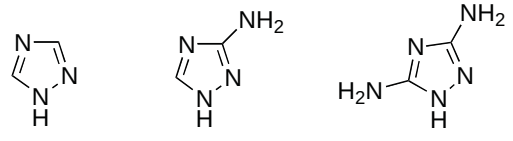

Scheme 1.

2. Experimental

2.1. General procedures

3,5-diamino-1,2,4-triazole (Am_2TAZ) and 1,2,4-triazole (TAZ) were purchased from Acros; zinc fluoride tetrahydrate was purchased from Strem Chemicals. All chemicals and reagents were used as received without further purification. Thermogravimetric analyses were carried out on a TA Instruments SDT 2960 simultaneous DTA-TGA by heating the samples at a rate of 5 °C/min in air. X-ray powder diffraction (XRD) patterns for Rietveld analysis were acquired on a Rigaku D/Max-2100 powder X-ray diffractometer with monochromatic Cu$K\alpha$ radiation ($\lambda = 0.15418$ nm). High temperature powder X-ray diffraction patterns were collected using a Rigaku hot stage attachment.

2.2. Preparation of [ZnF(Am_2TAZ)] · solvents

In a typical synthesis, 0.2 g (2 mmol) of Am_2TAZ, 0.35 g (2 mmol) of zinc fluoride tetrahydrate and 10 mL of water were placed into a 23 mL Teflon lined autoclave. The resulting mixture was stirred for 5 min prior to sealing the autoclave. The autoclave was then placed in a programmable furnace and heated to 160 °C at 1 °C/min and held at that temperature for 3 days. The mixture was then cooled to 60 °C at 0.1 °C/min and kept at 60 °C for 1 day before the furnace was shut off. White polycrystalline powder, which was phase pure by powder X-ray diffraction, was isolated from the reaction. Yield: 79%.

2.3. Preparation of [ZnF(TAZ)] · solvents

In a typical synthesis, 0.14 g (2 mmol) of TAZ, 0.35 g (2 mmol) of zinc fluoride tetrahydrate and 10 mL of water were placed in a 23 mL Teflon-lined autoclave. The resulting mixture was stirred for 5 min prior to sealing the autoclave. The autoclave was then placed in a programmable furnace and heated to 160 °C at 1 °C/min and held at that temperature for 3 days. The mixture was then cooled to 60 °C at 0.1 °C/min and kept at 60 °C for 1 day before the furnace was shut off. Colorless needle-shaped crystals formed. Yield: 68%.

3. Single crystal structure determination of ZnF(TAZ) · solvents (1)

X-ray intensity data from a colorless bar were measured at 294(2) K on a Bruker SMART APEX

CCD-based diffractometer (Mo$K\alpha$ radiation, $\lambda = 0.71073$ Å) [11]. Raw data frame integration and Lp corrections were performed with SAINT+ [11]. Final unit cell parameters were determined by least-squares refinement of 4128 reflections with $I > 5\sigma(I)$ from the data set. Analysis of the data showed negligible crystal decay during collection. Direct methods structure solution, difference Fourier calculations and full-matrix least-squares refinement against F^2 were performed with SHELXTL [12].

The compound crystallizes in the trigonal crystal system in the space group $R\bar{3}c$ as determined by the pattern of systematic absences in the intensity data and by the successful solution and refinement of the data. There are five non-hydrogen atoms in the asymmetric unit of the framework (Zn1, F1, N1, N2, C1). All were refined anisotropically. The hydrogen atom H1 of the TAZ ligand was placed in the geometrically idealized position and included as a riding atom with a refined isotropic displacement parameter. Zn1, F1, and the TAZ ligand are all located on a two-fold axis of rotation. The disordered intrachannel solvent guests were treated as discussed previously [10]. Electron density peaks were added to the refinement as variable-occupancy oxygen atoms of water molecules and refined with a fixed isotropic displacement parameter of $U_{eq} = 0.10$ Å^2. Peaks were added until a flat difference map was achieved, and no occupancy was allowed to refine under 10%. It should be noted that the occupancy of the channel species is strongly correlated to the chosen isotropic displacement parameter. The water content from the X-ray refinement is therefore approximate. Crystal data, data collection parameters, and refinement statistics for ZnF(TAZ) · solvents are listed in Table 1. Atomic coordinates and thermal parameters, and selected interatomic distances and bond angles for **1** are collected in Tables 2 and 3.

4. Rietveld refinement of ZnF(Am_2TAZ) · solvents (2) using powder X-ray diffraction data

A polycrystalline sample of ZnF(Am_2TAZ) · solvents was ground into a fine powder and used for the collection of powder X-ray diffraction data. Measurements were collected on a Rigaku D/Max-2100 powder X-ray diffractometer from 5° to 90° (2θ angle) with 0.04° steps and counting times of 30 s/step. Structures based on powder data were refined using the Rietveld method as implemented in the program Rietica [13]. The single crystal structure of ZnF(AmTAZ) · solvents [10] was used as a model for the refinement of ZnF(Am_2TAZ) · solvents. The amine occupancy in the model was adjusted to reflect the existence of two amine groups on the Am_2TAZ ligand. The atomic positions of the Zn, F and the AmTAZ ligand were not refined and the

Table 1
Crystal data and structure refinement for ZnF(TAZ) · solvents

Empirical formula	C2 H2 F N3 O2.09 Zn	
Formula weight	185.81	
Temperature	294(1) K	
Wavelength	0.71073 Å	
Crystal system	Trigonal	
Space group	$R\bar{3}c$	
Unit cell dimensions	$a = 18.6011(7)$ Å	$\alpha = 90°$
	$b = 18.6011(7)$ Å	$\beta = 90°$
	$c = 9.9000(8)$ Å	$\gamma = 120°$
Volume	2966.5(3) Å^3	
Z	18	
Density (calculated)	1.872 mg/m^3	
Absorption coefficient	3.678 mm^{-1}	
Crystal size	0.14 × 0.08 × 0.05 × mm^3	
Theta range for data collection	2.19–28.26°	
Index ranges	$-24 \leqslant h \leqslant 24$, $-24 \leqslant k \leqslant 24$, $-13 \leqslant l \leqslant 13$	
Reflections collected	12,303	
Independent reflections	822 [R(int) = 0.0679]	
Completeness to theta = 28.26°	100.0%	
Absorption correction	None	
Refinement method	Full-matrix least-squares on F^2	
Data/restraints/parameters	822/0/59	
Goodness-of-fit on F^2	1.097	
Final R indices [$I > 2$sigma(I)]	$R_1 = 0.0270$, w$R_2 = 0.0716$	
R indices (all data)	$R_1 = 0.0332$, w$R_2 = 0.0738$	
Largest diff. peak and hole	0.370 and −0.426 e Å^{-3}	

Table 2
Atomic coordinates ($\times 10^4$) and equivalent isotropic displacement parameters ($Å^2 \times 10^3$) for ZnF(TAZ)·solvents

	x	y	z	U_{eq}
Zn(1)	3749(1)	3749(1)	2500	21(1)
F(1)	4094(1)	3333	833	29(1)
C(1)	3681(2)	2121(2)	3272(2)	27(1)
N(1)	3562(1)	2740(1)	3581(2)	25(1)
N(2)	3333	1493(1)	4167	26(1)
O(1)	5500(20)	3480(20)	4520(40)	100
O(2)	5932(9)	3349(10)	3716(14)	100
O(3)	5800(30)	4000(40)	960(60)	100
O(4)	6667	4900(20)	833	100
O(5)	5468(19)	3333	833	100
O(6)	5400(20)	3160(30)	−40(40)	100
O(7)	5630(30)	3670(50)	620(40)	100

U_{eq} is defined as one-third of the trace of the orthogonalized U^{ij} tensor.

Table 3
Selected bond lengths (Å) and angles (deg) for ZnF(TAZ)·solvents

Zn(1)–N(2)#1	2.006(3)
Zn(1)–N(1)	2.034(2)
Zn(1)–F(1)	2.0566(10)
C(1)–N(1)	1.312(3)
C(1)–N(2)	1.346(3)
N(1)–N(1)#5	1.374(4)
N(2)#1–Zn(1)–N(1)	123.12(6)
N(2)#1–Zn(1)–N(1)#2	123.11(6)
N(1)–Zn(1)–N(1)#2	113.76(12)
N(2)#1–Zn(1)–F(1)	91.80(3)
N(1)–Zn(1)–F(1)	90.96(6)
N(1)#2–Zn(1)–F(1)	87.08(7)
N(2)#1–Zn(1)–F(1)#3	91.79(3)
N(1)–Zn(1)–F(1)#3	87.08(7)
N(1)#2–Zn(1)–F(1)#3	90.95(6)
F(1)–Zn(1)–F(1)#3	176.41(6)
Zn(1)–F(1)–Zn(1)#4	119.93(10)

Symmetry transformations used to generate equivalent atoms:
#1 $y+1/3$, $-x+y+2/3$, $-z+2/3$, #2 y, x,$-z+1/2$, #3 $-y+2/3$, $x-y+1/3$, $z+1/3$.
#4 $-x+y+1/3$,$-x+2/3$, $z-1/3$, #5 $-x+2/3$, $-x+y+1/3$, $-z+5/6$.
#6 $x-y+1/3$, $x-1/3$, $-z+2/3$.

solvents in the channels were modeled using oxygen atoms. Both the atomic positions and atomic displacement parameters of the solvent oxygens were refined with the atomic displacement parameters constrained to be equal. When these were allowed to refine freely the calculations tended to diverge. The peak shapes were refined using a pseudo-Voigt function and the background was calculated using an automatic smoothing function based on 20 steps. The lattice parameters were allowed to refine without any constraints. The X-ray powder diffraction pattern with difference plot (observed–calculated) is shown in Fig. 1. Tick marks correspond to the allowed ZnF(Am_2TAZ) Bragg reflections. Rietveld and least-squares refinement results, atomic coordinates and thermal parameters, and selected bond distances and angles are presented in Tables 4–6, respectively.

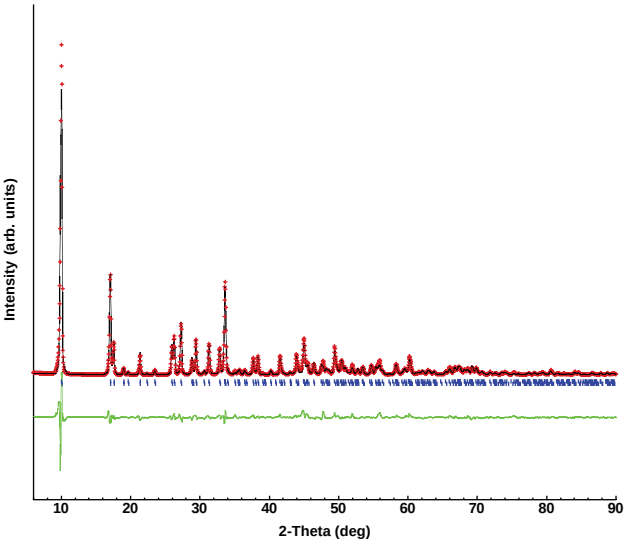

Fig. 1. Rietveld plot for ZnF(Am_2TAZ)·solvents. Observed (red) and calculated (black) X-ray diffraction profiles of ZnF(Am_2TAZ)·solvents at room temperature; a difference curve is shown (green). Vertical bars (blue) mark reflection positions for the ZnF(Am_2TAZ)·solvents phase.

Table 4
Summary of crystallographic data and least-squares refinement for ZnF(Am_2TAZ)·solvents

Space group	$R\bar{3}c$
a (Å)	18.508(1)
c (Å)	10.0376(8)
V ($Å^3$)	2977.9(3)
R_p (%)	11.9
R_{wp} (%)	15.8
R_{Bragg} (%)	10.88
χ^2	74

5. Results and discussion

Single crystals of ZnF(TAZ)·solvents and polycrystalline powders of ZnF(Am_2TAZ)·solvents (from hereon collectively referred to as ZnF(R_2TAZ)·solvents (R = H, NH_2)) were grown hydrothermally out of an aqueous solution containing zinc fluoride and the ligand (TAZ or Am_2TAZ) that was kept at 160 °C for 3 days. The crystals grow as needles and are the majority product in the case of the TAZ reaction, whereas the Am_2TAZ product is polycrystalline and seemingly phase

Table 5
Atomic coordinates ($\times 10^4$) and isotropic displacement parameters ($Å^2$) for ZnF(Am_2TAZ · solvents)

	x	*y*	*z*	*Biso*
Zn(1)	3755	3755	2500	3.6(1)
F(1)	4122	3333	833	3.1(3)
C(1)	3725	2149	3308	3.8(4)
N(1)	4297	2187	2348	3.6(3)
N(2)	3590	2767	3599	3.5(3)
N(3)	3333	1502	4167	5.3(3)
O(1)	5459(40)	2424(30)	1985(50)	34.4(7)
O(2)	3219(20)	2174(10)	1761(20)	34.4(7)
O(3)	5000	2197(20)	434(80)	34.4(7)
O(4)	6667	3333	1674(20)	34.4(7)
O(5)	5902(70)	3304(10)	3442(100)	34.4(7)
O(6)	4957(30)	2759(50)	9485(50)	34.4(7)
O(7)	5483(30)	4205(30)	513(50)	34.4(7)
O(8)	5701(30)	3606(50)	1112(100)	34.4(7)
O(9)	6456(20)	1380(20)	7698(50)	34.4(7)

Table 6
Selected bond lengths (Å) and angles (deg) for ZnF(Am_2TAZ) · solvents

Zn(1)–N(2)#1	2.0250(1)
Zn(1)–N(3)	1.9987(1)
Zn(1)–F(1)	2.0972(1)
C(1)–N(2)	1.3186(1)
C(1)–N(3)	1.3549(1)
N(2)–N(2)#5	1.4055(1)
N(3)#1–Zn(1)–N(2)	126.35
N(3)#1–Zn(1)–N(2)#2	126.38
N(2)–Zn(1)–N(2)#2	107.26
N(3)#1–Zn(1)–F(1)	91.38
N(2)–Zn(1)–F(1)	91.66
N(2)#2–Zn(1)–F(1)	86.88
N(3)#1–Zn(1)–F(1)#3	91.38
N(2)–Zn(1)–F(1)#3	86.88
N(2)#2–Zn(1)–F(1)#3	91.66
F(1)–Zn(1)–F(1)#3	177.23
Zn(1)–F(1)–Zn(1)#4	118.69

Symmetry transformations used to generate equivalent atoms:
#1 $y+1/3$, $-x+y+2/3$, $-z+2/3$, #2 y, x, $-z+1/2$, #3 $-y+2/3$, $x-y+1/3$, $z+1/3$.
#4 $-x+y+1/3$, $-x+2/3$, $z-1/3$, #5 $-x+2/3$, $-x+y+1/3$, $-z+5/6$.
#6 $x-y+1/3$, $x-1/3$, $-z+2/3$.

pure. In both cases a white solid impurity, believed to be Zn(OH)F, is sometimes observed. The synthesis conditions employed are very similar to those used in the original syntheses of ZnF(AmTAZ) · solvents by our group [10].

The framework structures of [ZnF(R_2TAZ)] are virtually identical to that of ZnF(AmTAZ), the differences arising from the presence of an additional amino group or conversely, the absence of all amino groups, on the triazole ligand. The framework structure consists of an extended, 3D tubular framework. The skeleton of the framework consists of a fundamental repeating unit [ZnF(R_2TAZ)], where the Zn and F atoms and the R_2TAZ ligand are located on two-fold rotational axes. Each Zn^{2+} center has a trigonal bipyramidal geometry with the three equatorial sites occupied by an imino nitrogen atom from three separate R_2TAZ ligands and the two apical positions occupied by F^- anions (Fig. 2). All three nitrogen atoms in the triazole (R_2TAZ) ring are coordinated to different Zn^{2+} centers; and the Zn^{2+} centers are further connected by F^- anions that act as μ_2-bridging atoms to link two neighboring Zn^{2+} centers. Thus, propagation of the structure in the crystal involves the μ_3-R_2TAZ units and the μ_2-F^- anions to generate a 3D framework containing large hexagonal channels (Fig. 3). In the case of the Am_2TAZ-based framework, the amino groups protrude into these channels, reducing their effective diameter. In the case of the ZnF(TAZ) framework, the amino groups are, of course, absent leaving a larger, more open channel.

Fig. 2a clearly shows the framework structure surrounding a single channel. The framework can be viewed as consisting of open-ended, hollow tubes extending along the *c*-axis with a crystallographically imposed $\bar{3}$ axis in the center of each tube. Consequently, as shown in Fig. 2a, each tube consists of hexanuclear metallamacrocycles made up of six ligands and six Zn^{2+} metal centers that are related by three-fold rotoinversion symmetry. Within this metallamacrocycle, each ligand utilizes its 1- and 4-positioned nitrogen donors to link two five-coordinate Zn^{2+} metal ions through two of the three equatorial sites. Each Zn^{2+} ion is further coordinated to another ligand with N–Zn–N angles of $\sim 123^\circ$ (Tables 3 and 6), enabling the joining of $\bar{3}$-symmetry related metallamacrocycles. Fusing of these metallamacrocycles via the third bridging ligand results in the honeycomb arrangement observed in the *ab* plane (Fig. 3). In addition, the 2-positioned nitrogen donor of each ligand is bound to one of the six Zn^{2+} centers belonging to an adjacent, hexanuclear metallamacrocycle (Fig. 2b). As shown in Fig. 4, stacking of the metallamacrocycles results in 1D chains running along the *c*-axis where connectivity is established via vertex sharing of ZnN_3F_2 polyhedra. Adjacent Zn^{2+} centers in these chains are part of 5-membered Zn_2N_2F rings, where each ring is composed of the two Zn^{2+} centers, a μ_2-bridging F^- anion and the 1- and 2-positioned bridging nitrogen atoms of the ligand. Overall, the ligand unit utilizes its 1- and 4-positioned nitrogen atoms to link trigonal bipyramidal Zn^{2+} centers into metallamacrocycles that are fused to generate a 2D honeycomb sheet in the *ab* plane. Such 2D sheets are connected in the third direction via bridging F^- anions and 2-positioned R_2TAZ nitrogen atoms to generate the 3D honeycomb tubular framework.

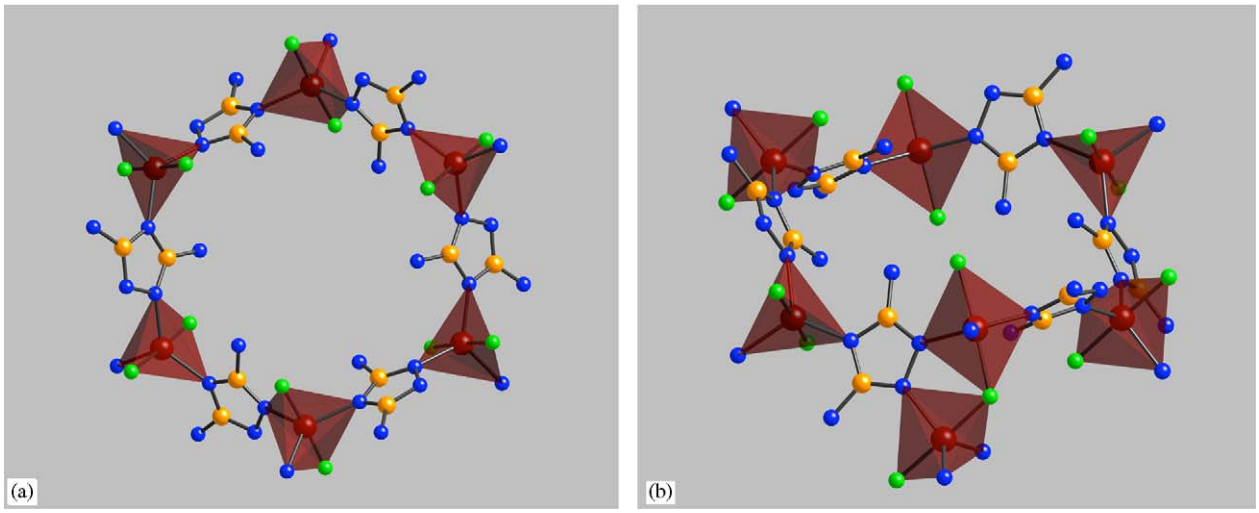

Fig. 2. (a) Three-fold symmetry related hexanuclear metallamacrocycle composed of six Am_2TAZ and six zinc centers. (b) View highlighting the connectivity between zinc centers and adjacent metallamacrocycles. Hydrogen atoms are omitted for clarity. Key: Zn, red; F, green; N, blue; C, yellow.

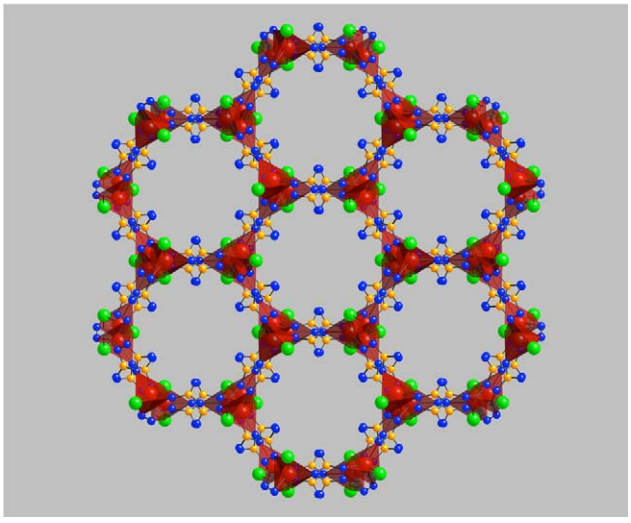

Fig. 3. Honeycomb tubular channels formed in the [ZnF(Am_2TAZ)] framework along the *c*-axis. The coordination geometry of the zinc centers is represented by red trigonal bipyramids. Hydrogen atoms are omitted for clarity. Key: Zn, red; F, green; N, blue; C, yellow.

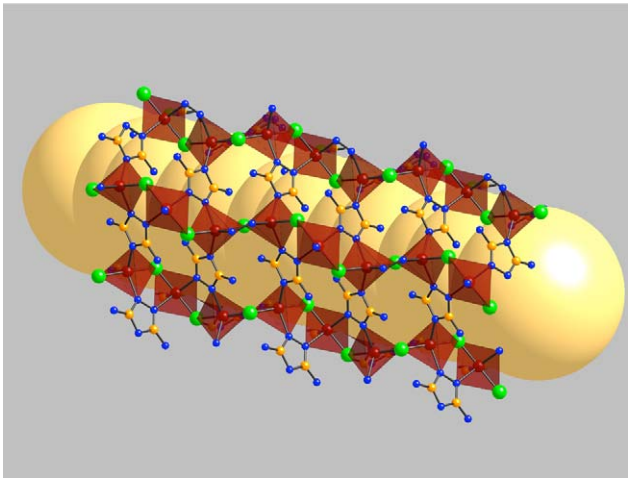

Fig. 4. Tubular structure of a single channel highlighting the connectivity of the zinc trigonal bipyramids and the connectivity of the Am_2TAZ ligand. The tube interior is represented by a yellow cylinder. Hydrogen atoms are omitted for clarity.

6. Structural robustness

The frameworks of ZnF(R_2TAZ) are very stable in air and can be heated to between 325 and 350 °C before the frameworks start to fall apart. This is similar to the thermal behavior observed for the previously reported ZnF(AmTAZ) framework and in all cases, the final decomposition product is ZnO, which begins to form when the samples are heated in air past 500 °C. TGA data collected in air exhibited an abrupt weight loss between 340 and 390 °C and between 380 and 430 °C, for ZnF(TAZ) · solvents and ZnF(Am_2TAZ) · solvents, respectively, indicating structure decomposition. This is confirmed by the high temperature XRD analyses, which indicate that the ZnF(TAZ) framework is stable until at least 300 °C while the ZnF(AmTAZ) and the ZnF(Am_2TAZ) frameworks remain intact to at least 335 °C. The high temperature XRD data is shown in Figs. 5 and 6 for ZnF(TAZ) · solvents and ZnF(AmTAZ) · solvents, respectively. As can be seen in Fig. 5, the main peaks for ZnF(TAZ) disappear at 335 °C, indicating the beginning of the structure decomposition. By comparison, the ZnF(Am_2TAZ) data, Fig. 6, indicates that the structure remains intact to at least 335 °C.

A fundamental question concerns the origin of the unusually high thermal stability of these channel-

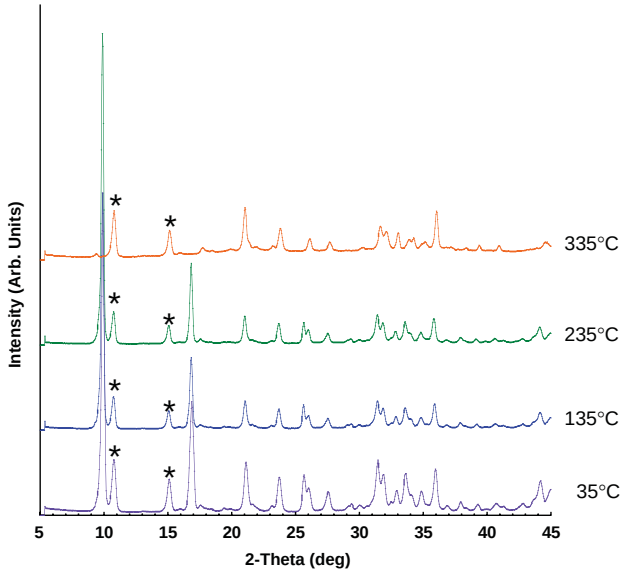

Fig. 5. Powder X-ray diffraction patterns of ZnF(TAZ)·solvents collected at 35, 135, 235, and 335 °C. Impurity peaks are marked by an asterix.

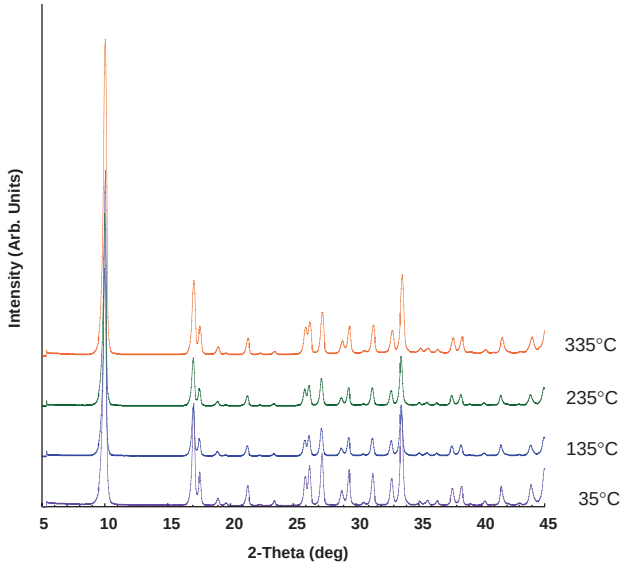

Fig. 6. Powder X-ray diffraction patterns of ZnF(Am_2TAZ)·solvents collected at 35, 135, 235, and 335 °C.

containing frameworks. One can hypothesize that the combination of strong Zn–F and Zn–N linkages, coupled with the small ligand size, is one reason for this high thermal stability. If this is the case, then one should be able to expand upon these structures and prepare other exceptionally thermally stable frameworks using related nitrogen containing heterocycles. An obvious extension of this work concerns the synthesis of the methyl derivatives of TAZ, MeTAZ and Me_2TAZ. These ligands would generate a much more hydrophobic channel environment and their syntheses and investigations are ongoing. Clearly, one can envision using other substituted triazoles as well as more complex nitrogen-containing heterocycles as ligands.

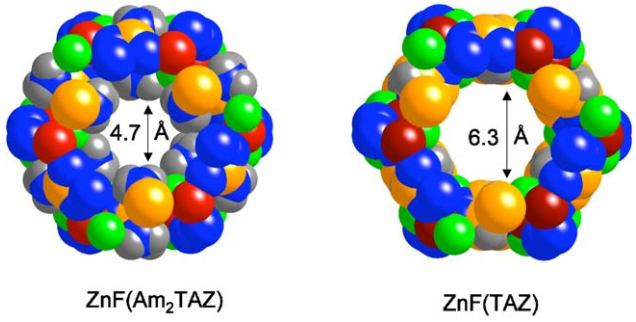

Fig. 7. Space filling view of single tubes of ZnF(TAZ)·solvents and ZnF(Am_2TAZ)·solvents highlighting the reduction in channel diameter due to the presence of amine groups in ZnF(Am_2TAZ)·solvents protruding into the channel. Atoms are drawn with appropriate van der Waals radii (C: 1.7 Å, H: 1.2 Å, N: 1.5 Å, F: 1.35 Å).

Another fundamental concern for framework structures is the ability to exercise control over the channel size. In the structures discussed in this paper, the nitrogen positions on the R_2TAZ group establish the Zn–N–C–N–Zn curvature in the metallamacrocycles, and thereby determine its ring size. Increasing the curvature with a hypothetical Zn–N–C–C–N–Zn sequence (by using a six membered heterocyclic ring) may lead to a larger metallamacrocycle with greater channel diameter. Again, one can envision other nitrogen-containing heterocycles that could potentially achieve this goal.

The channel size (in the present framework structures) is sensitive to the substituents on the triazole ligand, and these substituents also control the chemical environment in the channels. As shown in Fig. 7, where space filling representations of the channels in both the ZnF(TAZ) and the ZnF(Am_2TAZ) frameworks are depicted, the presence of the two amine groups in the ZnF(Am_2TAZ) framework reduces the channel diameter from ~6.3 Å in the ZnF(TAZ) framework to only ~4.7 Å in the ZnF(Am_2TAZ) framework. Clearly, it is desirable to achieve larger channel diameters by employing more favorable ligand geometries as discussed above. This would increase the available space in the channel and thus provide sufficient room to accommodate even bulky substituents on the triazole ligand without completely filling the channel. This work, to control the hydrophobicity in larger channel structures, is currently ongoing.

7. Conclusion

Two new, exceptionally thermally stable, hollow tubular metal–organic architectures, [ZnF(TAZ)]·solvents and [ZnF(Am_2TAZ)]·solvents have been

synthesized and structurally characterized. The framework structures of both compounds are thermally stable to over 300 °C. A strategy for synthesizing other thermally stable porous framework structures has been presented along with a suggestion on controlling the hydrophobicity of the channel environment.

8. Supplementary materials

X-ray crystallographic data in CIF format for complex **1** has been deposited with the Cambridge Crystallographic Data Centre. The deposit number is CCDC-266086.

Acknowledgments

This research was supported by the National Science Foundation through Grant CHE:0314164.

Reference

[1] (a) A.K. Cheetham, G. Ferey, T. Loiseau, Angew. Chem. Int. Ed. 38 (1999) 3269;
(b) M. Eddaoudi, D.B. Moler, H.L. Li, B.L. Chen, T.M. Reineke, M. O'Keeffe, O.M. Yaghi, Acc. Chem. Res. 34 (2001) 319;
(c) J.D. Hartgerink, T.D. Clark, M.R. Ghadiri, Chem. Eur. J. 4 (1998) 1367;
(d) C.N.R. Rao, M. Nath, Dalton Trans. 1 (2003);
(e) A. Corma, Chem. Rev. 97 (1997) 2373;
(f) F. Schuth, W. Schmidt, Adv. Mater. 14 (2002) 629;
(g) A. Stein, Adv. Mater. 15 (2003) 763.

[2] (a) S.S.Y. Chui, S.M.F. Lo, J.P.H. Charmant, A.G. Orpen, I.D. Williams, Science 283 (1999) 1148;
(b) P.J. Hagrman, D. Hagrman, J. Zubieta, Angew. Chem. Int. Ed. 38 (1999) 2639;
(c) B.L. Chen, M. Eddaoudi, S.T. Hyde, M. O'Keeffe, O.M. Yaghi, Science 291 (2001) 1021;
(d) G.B. Gardner, D. Venkataraman, J.S. Moore, S. Lee, Nature 374 (1995) 792.

[3] (a) M. Eddaoudi, J. Kim, N. Rosi, D. Vodak, J. Wachter, M. O'Keefe, O.M. Yaghi, Science 295 (2002) 469;
(b) S. Noro, S. Kitagawa, M. Kondo, K. Seki, Angew. Chem. Int. Ed. 39 (2000) 2082.

[4] M. Eddaoudi, H.L. Li, O.M. Yaghi, J. Am. Chem. Soc. 122 (2000) 1391.

[5] (a) N.G. Pschirer, D.M. Ciurtin, M.D. Smith, U.H.F. Bunz, H.C. zur Loye, Angew. Chem. Int. Ed. 41 (2002) 583;
(b) N.L. Rosi, M. Eddaoudi, J. Kim, M. O'Keeffe, O.M. Yaghi, Angew. Chem. Int. Ed. 41 (2001) 284;
(c) K. Biradha, Y. Hongo, M. Fujita, Angew. Chem. Int. Ed. 39 (2000) 3843.

[6] X.L. Xu, M. Nieuwenhuyzen, S.L. James, Angew. Chem. Int. Ed. 41 (2002) 764.

[7] (a) O.M. Yaghi, C.E. Davis, G.M. Li, H.L. Li, J. Am. Chem. Soc. 119 (1997) 2861;
(b) I. Goldberg, Chem-Eur. J. 6 (2000) 3863.

[8] (a) J. Kim, B.L. Chen, T.M. Reineke, H.L. Li, M. Eddaoudi, D.B. Moler, M. O'Keeffe, O.M. Yaghi, J. Am. Chem. Soc. 123 (2001) 8239;
(b) C.Y. Su, X.P. Yang, B.S. Kang, T.C.W. Mak, Angew. Chem. Int. Ed. 40 (2001) 1725;
(c) J.S. Seo, D. Whang, H. Lee, S.I. Jun, J. Oh, Y.J. Jeon, K. Kim, Nature 404 (2000) 982;
(d) S.A. Bourne, J.J. Lu, A. Mondal, B. Moulton, M.J. Zaworotko, Angew. Chem. Int. Ed. 40 (2001) 2111.

[9] H. Li, M. Eddaoudi, M. O'Keeffe, O.M. Yaghi, Nature 402 (1999) 276.

[10] C.-Y. Su, A.M. Goforth, M.D. Smith, P.J. Pellechia, H.-C. zur Loye, J. Am. Chem. Soc. 126 (2004) 3576–3586.

[11] SMART Version 5.625, SAINT+ Version 6.22, Bruker Analytical X-ray Systems, Inc., Madison, Wisconsin, USA, 2001.

[12] G.M. Sheldrick, SHELXTL Version 6.1, Bruker Analytical X-ray Systems, Inc., Madison, Wisconsin, USA, 2000.

[13] B.A. Hunter, C.J. Howard, Rietica, v. 1.7.7, http://www.rietica.org, Lucas Heights Research Laboratories, N.S.W., Australia, 1997.